Magazine of Concrete Research
Volume 65 Issue 9

Scaling of fracture and acoustic emission in concrete
Invernizzi, Lacidogna and Carpinteri

Magazine of Concrete Research, 2013, **65**(9), 529–534
http://dx.doi.org/10.1680/macr.12.00112
Paper 1200112
Received 12/07/2012; revised 19/10/2012; accepted 09/11/2013
Published online ahead of print 13/03/2013

ice
Institution of Civil Engineers
publishing

Scaling of fracture and acoustic emission in concrete

Stefano Invernizzi
Dipartimento di Ingegneria Strutturale, Edile e Geotecnica, Politecnico di Torino, Corso Duca degli Abruzzi, Torino, Italy

Giuseppe Lacidogna
Dipartimento di Ingegneria Strutturale, Edile e Geotecnica, Politecnico di Torino, Corso Duca degli Abruzzi, Torino, Italy

Alberto Carpinteri
Dipartimento di Ingegneria Strutturale, Edile e Geotecnica, Politecnico di Torino, Corso Duca degli Abruzzi, Torino, Italy

A combined compression and acoustic emission (AE) test is proposed to study the scaling of fracture and AE in concrete-like specimens with different size and slenderness. The cylindrical concrete specimens were drilled from two pilasters sustaining an Italian viaduct built in the 1950s. A finite-element method model of the pure compression tests is presented, which is able to describe both the discrete cracking at the matrix–aggregate interface and the smeared cracking of the matrix. The adopted mesoscale modelling directly accounts for the aggregate dimensional distribution, each aggregate being explicitly represented. In this way, the crack patterns can be simulated correctly, as well as the load–displacement curve. During microcrack propagation, AE events can be clearly detected experimentally. Therefore, the number of AE can be put into relation with the number of Gauss points in the finite-element model where cracking takes place. A good correlation is found between the amount of cracking simulated numerically and the experimental AE counting number for different specimen sizes, and the two quantities show the same scaling exponent. This evidence reconfirms the assumption, provided by fragmentation theories, that the energy dissipation during microcrack propagation occurs in a fractal domain.

Notation

D	fractal exponent
d	diameter of the sample
E	Young's modulus
f_c	compressive strength
f_t	tensile strength
G_f	fracture energy
h	height of the sample
N_{max}	critical number of acoustic emission cumulative events at the peak stress
$N_{max,r}$	critical number of acoustic emission cumulative events of the reference specimen at the peak stress
V	volume
V_r	volume of the reference specimen
W_{max}	total dissipated energy
Γ	fractal energy density
Γ_{AE}	fractal acoustic emission event density
λ	slenderness of the sample
ν	Poisson ratio
σ_u	peak stress

Introduction

Non-destructive and instrumental investigation methods are currently employed to measure and check the evolution of adverse structural phenomena, such as damage and cracking, and to predict their subsequent developments. The choice of a technique for controlling and monitoring reinforced concrete or masonry structures is strictly correlated with the kind of structure to be analysed and the data to be extracted (Anzani *et al.*, 2000; Carpinteri and Bocca, 1991).

This study addresses the pure compression test carried out in the laboratory performed on drilled concrete cores obtained from two pilasters sustaining a viaduct along an Italian highway (Carpinteri *et al.*, 2007a). At the same time, the cracking processes taking place during the test were monitored using the acoustic emission (AE) technique. A similar approach has already been exploited in Carpinteri *et al.* (2007b), in an attempt to link the amount of AE with the structural deflections.

In the assessment of structural integrity, the AE technique has proved particularly effective (Carpinteri *et al.*, 2007b; Carpinteri and Lacidogna, 2006a, 2006b), in that it makes it possible to estimate the amount of energy released during the fracture process and to obtain information on the criticality of the process underway. The energy dissipated by the monitored structure is strictly connected to the energy detected by AE. The energy dissipated during crack formation in structures made of quasi-brittle materials plays a fundamental role in the behaviour throughout their life. Recently, according to fractal concepts, an ad hoc theory has been employed to monitor structures by means of the AE technique (Carpinteri *et al.*, 2007a, 2007b; Carpinteri and Lacidogna, 2006a, 2006b). The fractal theory takes into account the multiscale character of energy dissipation and the

strong size effects associated with it. With this energetic approach, it becomes possible to introduce a useful damage parameter for structural assessment based on a correlation between AE activity in the structure and the corresponding activity recorded on specimens of different sizes, tested to failure by means of double flat-jacks or pure compression tests. The main achievement of the present work consists in showing how the amount of cracking obtained from the numerical simulation and the AE events share the same scaling laws.

Combined compression and AE tests

By means of the AE technique, the damage evolution in two pilasters sustaining a viaduct along an Italian highway built in the 1950s was analysed. From the pilasters, some concrete cylindrical specimens were drilled in order to detect the mechanical properties of the material under compression and to evaluate the scale effects in size and time on AE activity (Carpinteri *et al.*, 2007a).

Test specimens and testing equipment

The cementitious material, of rather good mechanical characteristics, presents an apparent specific weight of about 2·22 g/cm^3 and a maximum aggregate size of about 15 mm. For each pilaster, three different specimen diameters d are considered in a maximum scale range of 1:3·4. The specimens present three different slendernesses: $\lambda = h/d = 0{\cdot}5$, 1·0 and 2·0, with d chosen equal to 27·7, 59, 94 mm, respectively. For each of these nine geometries, three specimens have been tested, for a total of 54 cases (two pilasters). The average values obtained from the experimental data are reported in Table 1. The system adopted in the compression test uses rigid steel platens, the lateral deformation of concrete being therefore confined at the specimen ends, which are forced to have the same lateral deformation as the rigid platens (see Figure 1).

The stress and cumulated event number plotted against time for a specimen of intermediate size is represented in Figure 2. In the figure the critical number of AE cumulative events N_{max} is represented in correspondence of the peak stress σ_u. Similar results can be observed in the other cases.

Figure 1. Apparatus adopted for compression tests

Numerical results

The numerical models of the pure compression tests were built accounting for the presence of aggregates and of the cementitious matrix. Quadratic elements were used to represent both the aggregates and the matrix, while special interface elements were

Specimen type	Diameter d: mm	Slenderness $\lambda = h/d$	Experimental peak stress: MPa	N_{max} at σ_u	Numerical peak stress: MPa
C11	27·7	0·5	91·9	1186	46·9
C12	27·7	1·0	62·8	1191	48·0
C13	27·7	2·0	48·1	1188	46·2
C21	59·0	0·5	68·1	8936	45·8
C22	59·0	1·0	53·1	8934	47·8
C23	59·0	2·0	47·8	8903	47·5
C31	94·0	0·5	61·3	28 502	46·4
C32	94·0	1·0	47·8	28 721	46·1
C33	94·0	2·0	44·1	28 965	45·9

Table 1. Experimental values obtained on concrete samples from pilaster P1

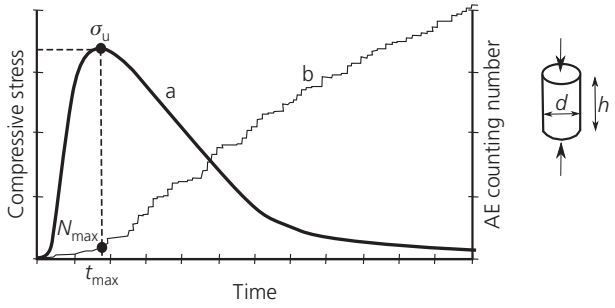

Figure 2. Stress and cumulated event number against time. a: is compressive stress; b: AE counting number

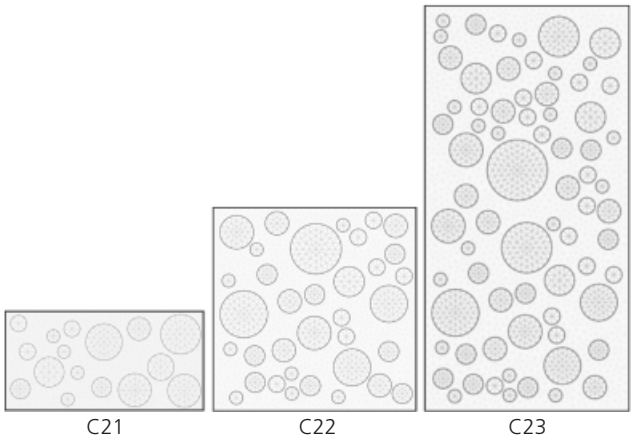

Figure 3. Three meshes of the modelled specimens

placed in between the two phases. The adopted mesoscale modelling directly accounts for the aggregate dimensional distribution, each aggregate being explicitly represented. The failure of the two phases was assumed as being driven by plasticity in compression, with parabolic relation, and by linear softening in tension. A rotating smeared crack model based on total deformation was used. To avoid mesh dependency, the constitutive law for continuum elements is regularised providing that the area beneath the stress strain diagram in tension is equal to the tensile fracture energy divided by the crack bandwidth (i.e. the element size). The constitutive relation for interfaces was assumed elastic in compression and linear softening in tension. As the constitutive law for interface elements is directly formulated in terms of stress against crack opening displacement (i.e. a cohesive law is assigned), no further regularisation is necessary. All the analyses were performed with the finite-element software Diana 9·2 (de Witte and Schreppers, 2007). The distribution of aggregate size and position was generated with the help of the module Lattice of the program, according to the Füller distribution. The mechanical properties of the materials are summarised in Table 2. Figure 3 shows the mesh used to model the C2(1–3) specimens.

Figure 4(a) shows the boundary conditions and the load scheme of one of the specimens. Perfect friction between the loading platens and the specimen was assumed. In order to control the loading scheme with the arc-length algorithm, only the horizontal displacements of the top of the specimen were fixed, while the vertical displacements were kept equal by means of additional tying constrains. Figure 4(b) shows the typical barrel-shaped deformed mesh that is obtained under the above assumptions.

Figure 5 shows the load–displacement curve obtained for the specimen C22. In general, accounting for cracking only it is not sufficient to simulate the peak load correctly, and the crushing of the matrix has necessarily to be taken into consideration. For this reason, the compressive behaviour of the matrix is assumed as elastic perfectly plastic. On the other hand, the simulation of the post-peak branch of the load–displacement curve is cumbersome, and many convergence issues arise. Fortunately, the post-peak regime was not of prior interest for the following analyses.

Figure 6 shows the localisation of the matrix crushing in correspondence of the zones comprised among the most loaded aggregates. The crushed zones reveal sub-vertical patterns, similar to what is observed for cracking.

The crack pattern for the three C2(1–3) samples is shown in Figure 7. It slightly changes varying the size, according to the different aspect ratios.

Comparison between fracture and AE scaling

In previous works (Carpinteri *et al.*, 2007a, 2007b; Carpinteri and Lacidogna, 2006a), a statistical and fractal analysis of data from

		Aggregate	Matrix	Interface
Young's modulus	E	$7{\cdot}0 \times 10^9$ Pa	$2{\cdot}5 \times 10^9$ Pa	$10{\cdot}0 \times 10^9$ N/m
Poisson ratio	ν	0·15	0·15	—
Tensile strength	f_t	$10{\cdot}0 \times 10^6$ Pa	$5{\cdot}0 \times 10^5$ Pa	$2{\cdot}0 \times 10^5$ Pa
Fracture energy	G_f	60 N/m	6 N/m	3 N/m
Compressive strength	f_c	—	5×10^7 Pa	—

Table 2. Mechanical properties adopted in the analysis

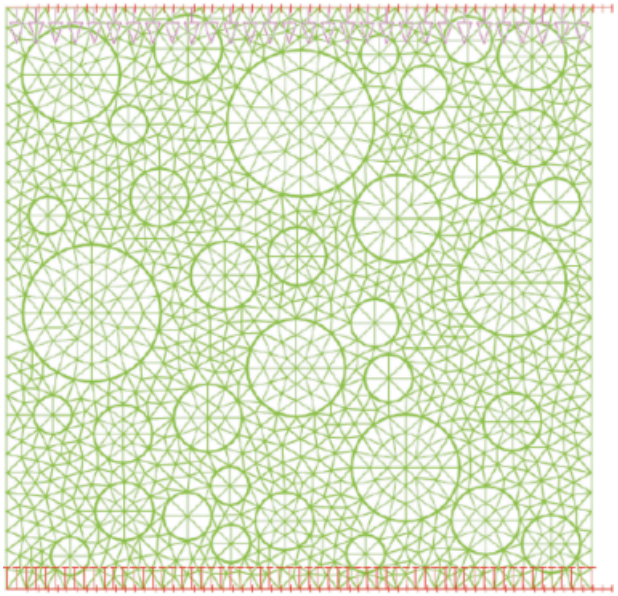

(a)

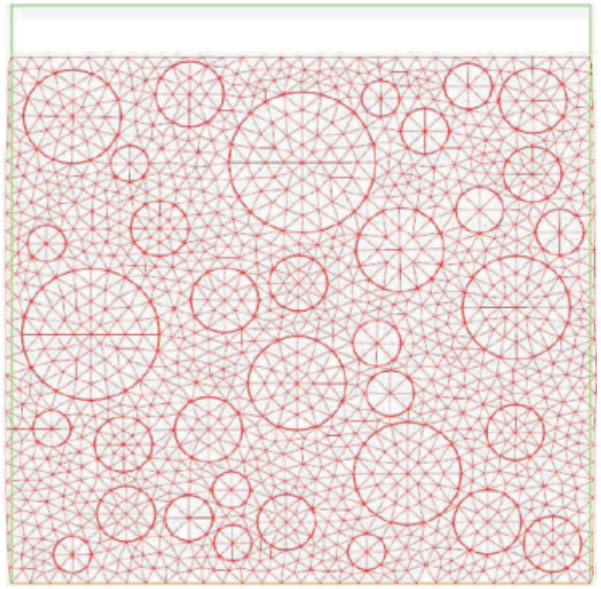

(b)

Figure 4. Loading scheme and boundary condition of (a) specimen C22 and (b) deformed shape

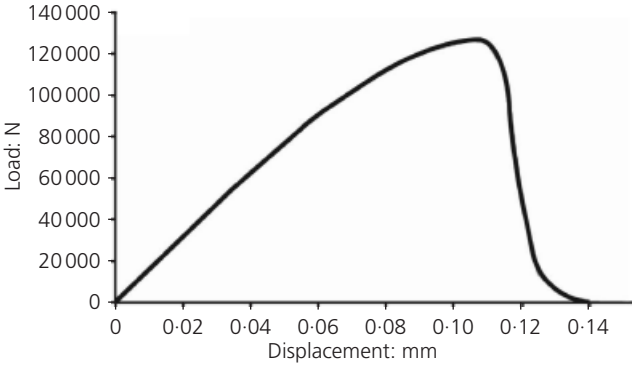

Figure 5. Load–displacement curve

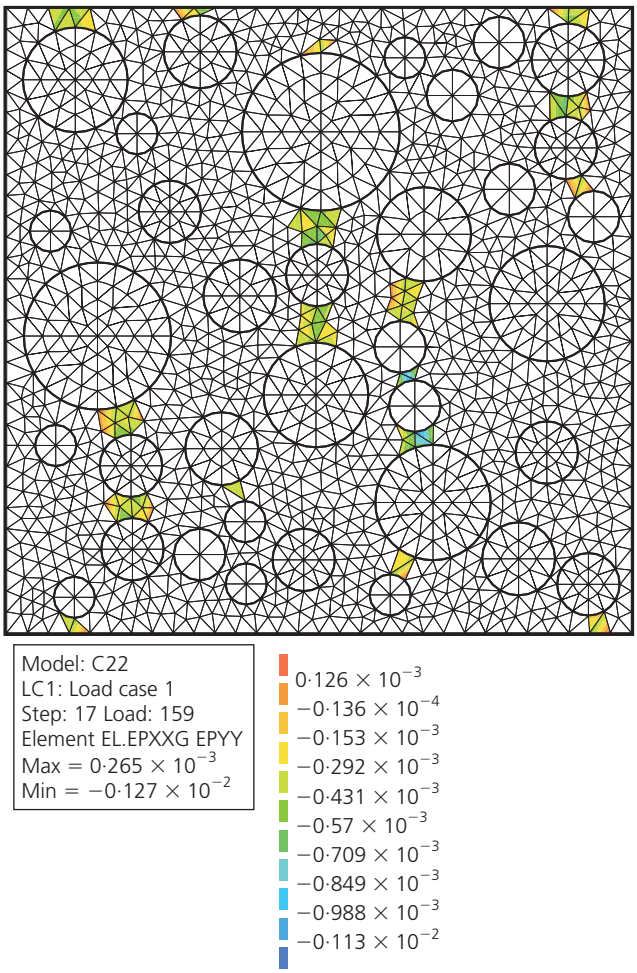

Figure 6. Crushing in the matrix of the specimen C22

laboratory experiments was performed, considering the multiscale aspect of cracking phenomena. The fractal criterion takes into account the multiscale character of energy dissipation and the strong size effects associated with it. This makes it possible to introduce a useful energy-related parameter for the damage determination of full-size structure, by comparing the AE monitoring results with the values obtained on a reference specimen sampled from the structure and tested up to failure. This approach has been exploited by the authors for the interpretation of double flat-jack tests performed in historical masonry walls (ASTM, 1991; Carpinteri *et al.*, 2009; Sacchi Landriani and Taliercio, 1986).

Fragmentation theories have shown that, during microcrack propagation, energy dissipation occurs in a fractal domain between a surface and the specimen volume V (Carpinteri and Pugno, 2002). This implies that a fractal energy density (having anomalous physical dimensions)

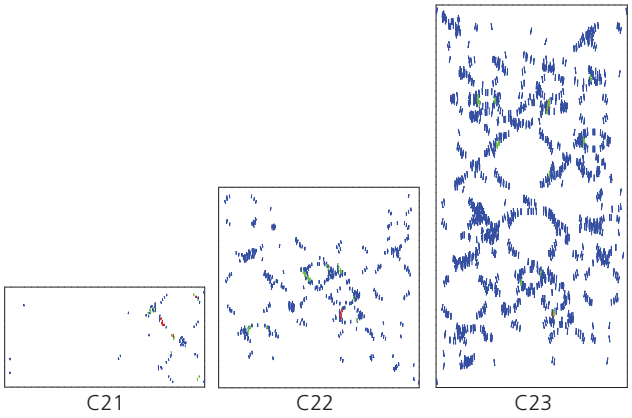

Figure 7. Crack patterns in specimens C12, C22 and C23

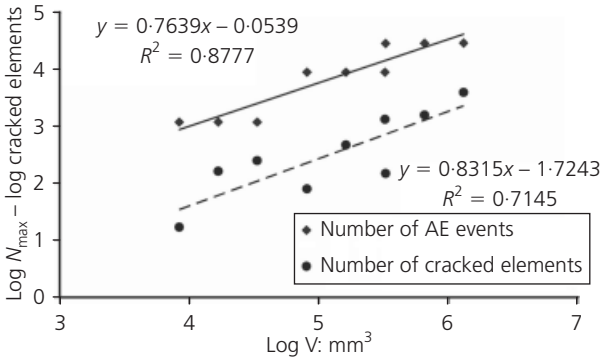

Figure 8. Scale effect on N_{max} and on the number of cracked finite elements

1. $$\Gamma = \frac{W_{max}}{V^{D/3}}$$

can be considered as the size-independent parameter. In the fractal criterion of Equation 1, W_{max} = total dissipated energy, Γ = fractal energy density and D = fractal exponent that is comprised between 2 and 3.

On the other hand, during microcrack propagation, AE events can be clearly detected. As the energy dissipated, W is proportional to the number of the oscillations counts N, related to the AE events, Γ_{AE} can be considered as a size-independent parameter

2. $$\Gamma_{AE} = \frac{N_{max}}{V^{D/3}}$$

where Γ_{AE} is fractal AE event density; and N_{max} is evaluated at the peak stress, σ_u. Equation 2 predicts a volume effect on the maximum number of AE events for a specimen tested up to the peak stress.

The extent of structural damage in a full-size structure can be worked out from the AE data recorded on a reference specimen (subscript r) obtained from the structure. From Equation 2 we obtain

3. $$N_{max} = N_{max,r}\left(\frac{V}{V_r}\right)^{D/3}$$

from which the structure critical number of AE events N_{max} can be obtained.

Now, we can verify that the AE counting number is also proportional to the number of Gauss points subjected to cracking in the finite-element model. Therefore, the number of AE and the number of cracks in the finite-element model should show the same exponent with respect to the considered volume. In fact, this is what we can substantially observe from Figure 8 considering the nine different specimens. For these reasons, it is possible to say that the numerical model is able to describe correctly the decrease in crack density with increasing specimen size.

Finally, let us observe that the intercept of this relation depends on the discretisation of the finite-element model. On the other hand, refining the mesh does not change sensibly the exponents reported in Figure 8.

Conclusions

A numerical simulation of an innovative concrete compression test combined with AE monitoring has been proposed. The numerical results agree rather well with the experimental evidence, and the crack patterns are simulated correctly. On the other hand, the model is not able to describe the decrease of the overall strength with increasing size, probably owing to the introduction of the limit compression strength to model the crushing of the matrix, or to more fundamental reasons.

In addition, the number of AE is compared with the number of Gauss points in the finite-element model where cracking takes place. A good correlation is found between the amount of cracking simulated numerically and the experimental AE counting number for different specimen sizes.

Although it is impossible easily to obtain a direct relation between the AE and the amount of cracking, it is possible to state that the two quantities are proportional to each other when increasing sizes are considered.

REFERENCES

Anzani A, Binda L and Mirabella Roberti G (2000) The effect of heavy persistent actions into the behavior of ancient masonry. *Materials and Structures* **33(228)**: 251–261.

ASTM (1991) C1197-91: Standard test method for in situ

measurement of masonry deformability properties using the flat-jack method. ASTM International, West Conshohocken, PA, USA.

Carpinteri A and Bocca P (1991) *Damage and Diagnosis of Materials and Structures*, Pitagora Editrice, Bologna, Italy.

Carpinteri A and Lacidogna G (2006a) Structural monitoring and integrity assessment of medieval towers. *Journal of Structural Engineering (ASCE)* **132(11)**: 1681–1690.

Carpinteri A and Lacidogna G (2006b) Damage monitoring of a masonry building by the acoustic emission technique. *Materials and Structures* **39(2)**: 161–167.

Carpinteri A and Pugno N (2002) Fractal fragmentation theory for shape effects of quasi-brittle materials in compression. *Magazine of Concrete Research* **54(6)**: 473–480.

Carpinteri A, Lacidogna G and Pugno N (2007a) Structural damage diagnosis and life-time assessment by acoustic emission monitoring. *Engineering Fractures Mechanics* **74(1–2)**: 273–289.

Carpinteri A, Invernizzi S and Lacidogna G (2007b) Structural assessment of a XVIIth century masonry vault with AE and numerical techniques. *International Journal of Architectural Heritage* **1(2)**: 214–226.

Carpinteri A, Invernizzi S and Lacidogna G (2009) Historical brick-masonry subjected to double flat-jack test: acoustic emissions and scale effects on cracking density. *Construction and Building Materials* **23(8)**: 2813–2820.

de Witte FC and Schreppers GJ (2007) *DIANA Finite Element Analysis User's Manual*. TNO Diana BV, Delft, The Netherlands.

Sacchi Landriani G and Taliercio A (1986) Numerical analysis of the flat jack test on masonry walls. *Journal of Theoretical and Applied Mechanics* **5(3)**: 313–339.